Received September 6, 2019, accepted September 17, 2019, date of publication September 24, 2019,
date of current version October 4, 2019.

Digital Object Identifier 10.1109/ACCESS.2019.2943411

Commutation Torque Ripple Reduction for Brushless DC Motor Based on an Auxiliary Step-Up Circuit

XULIANG YAO, JICHENG ZHAO, JINGFANG WANG, SHENGQI HUANG, AND YISHU JIANG
College of Automation, Harbin Engineering University, Harbin 150001, China
Corresponding author: Jicheng Zhao (worryfree@126.com)

ABSTRACT There exists torque ripple in the commutation process of brushless DC motor (BLDCM), which seriously restricts its application in the high-performance field. This paper proposes an auxiliary step-up circuit to suppress the commutation torque ripple of BLDCM, and the auxiliary step-up circuit consists of a transformer, a capacitor and a switch circuit. For effective suppression of the commutation torque ripple, the capacitor is charged in the non-commutation period. When the commutation occurs, the charged capacitor is added on the power source through a switch circuit to step up the dc-bus voltage in the commutation period, and the three-phase inverter is regulated to make the motor's input voltage is equal to four times the back electromotive force (back EMF) amplitude. The auxiliary step-up circuit only transfers partial power required in the commutation process of the motor, and the capacity of the power components is reduced accordingly. The inductive energy stored in the transformer is returned to the power source in each switching cycle, which improves the energy utilization rate. In addition, this method can also shorten the commutation time. The validity and effectiveness of the proposed method is verified through experimental results.

INDEX TERMS Brushless DC motor, commutation torque ripple, dc-bus voltage, commutation time.

I. INTRODUCTION

Brushless DC motor (BLDCM) is often one of the candidates for motion control due to the advantages of high efficiency, better reliability and lower maintenance cost [1], [2]. Compared with SPMSM, BLDCM has higher power density and lower cost. However, it causes larger torque ripple due to the inherent structure and specific supply mode [3]–[5]. The commutation torque ripple caused by the structure characteristics and the control strategy might generate mechanical vibration and noise. The maximum relative torque ripple reaches up to 50% of the average torque in the high-speed range [6], which have already restricted the applications in the high-performance field significantly. Therefore, the torque ripple reduction is important to improve the motor performance [7]. Up to now, the research on the suppression of the commutation torque ripple has attracted extensive attention over the past decades [8], [1].

Recently, suppression strategies for the commutation torque ripple have been widely investigated. Among various control methods, they can mainly be divided into three types according to the control variables. The first method is based on the current control. In [9], a suppression technique of the commutation torque ripple with a single DC current sensor is proposed. In this method, the torque ripple is decreased by equalizing the mismatched slopes of the incoming and outgoing phase currents during the commutation period. The control method combined with PWM_ON_PWM is proposed to suppress the commutation torque ripple in [10], and the effect of the diode freewheeling on the torque is considered. In [11], the authors propose a three-segment modulation method to eliminate the torque ripple. In this method, each PWM period is divided in three separate parts during the commutation period, which makes the commutation time controllable. A current optimization control method is proposed to reduce the torque ripple in [12], where the integral variable structure control is used to improve the robustness of the controller. In [13], the PWM theme is applied to the non-commutation phase during the commutation period, and the torque ripple is compensated by equalizing the disturbed average voltage of the non-commutated phase before and after commutation. The finite-state model predictive control is also introduced

The associate editor coordinating the review of this manuscript and approving it for publication was Xiaodong Sun.

to minimize the torque ripple in [14], and the optimal conduction state of the next cycle is obtained directly from the cost function which accelerates the dynamic response. The coordinate transformation is proposed to reduce the commutation torque ripple in [15]. In [16], the harmonic current injection and sliding mode control are jointly used to control the torque. The experimental results show that the method has the favorable dynamic performance and strong robustness.

The second method involves using the torque as the control variable. In [17], the PWM strategy based on the actual back EMF is employed to keep the average torque constant during the normal conduction and the commutation period, and the effect of the limited dc-bus voltage is also considered. In [18], an improved direct torque controller is designed to attenuate the torque ripple, and the operation mode in the commutation period is adaptively determined by the torque difference, which improves the dynamic characteristic of the torque. In [19], a sensorless direct torque control (DTC) method is proposed for saliency BLDCM. In this method, the stator current estimator and phase-locked loop are used to estimate the electromagnetic torque. The operation performance and the robustness to load variation are improved, and the stable minimum speed reaches as low as 33r/min. In terms of the characteristic of the field-oriented control and DTC, a hybrid control scheme is proposed for sensorless BLDCM in [20]. The proposed method has strong robustness against parameter uncertainties and is applicable in a wide speed range. In [21], two switching tables composed of the main vector and auxiliary vector are constructed depending on the torque slope, and the torque ripple caused by both the nonideal back EMF and current commutation are effectively mitigated with the combination of the two types of vectors. In [22], a single-cycle torque control algorithm is proposed to suppress the torque ripple of the motor. In this study, the unit cycle power is used as the feedback torque to make the average torque follow the reference torque, which suppresses the torque ripple and reduces the complexity of hardware implementation. The commutation torque ripple generated in the high-speed range is effectively reduced with the suppression methods above, but the unfavorable commutation time is extended due to the fixed dc-bus voltage.

The third method is to adjust the dc-bus voltage of the commutation period. To suppress the commutation torque ripple, various DC/DC converters are also introduced to obtain the desirable dc-bus voltage for suppression of the commutation torque ripple. In [23], a buck converter is added in front of the three-phase inverter. The regulation function of the dc-bus voltage is achieved by controlling the duty cycle of the converter. The proposed method works well in the low-speed range. The authors in [24] propose a voltage regulating circuit combining the H-bridge and the LRC circuit for a single-phase BLDC motor. The results show that the acoustic noise and the commutation torque ripple are obviously weakened. In [25], the dc-bus voltage is regulated by the power source in the non-commutation period and is switched to a single-ended primary inductor converter (SEPIC) in the commutation period. With this switching method, the torque ripple produced in the commutation period is effectively reduced. In [26], the modified SEPIC converter and a three-level neutral-point-clamped inverter are combined to regulate the dc-bus voltage. With the mixed structure, the resultant torque ripple is mitigated and the harmonic components are further lowered. The Z-source inverter is also applied in [27], where the commutation torque ripple is eliminated by regulating the shoot-through vector and active vector duty cycles, and the results show that the torque ripple is reduced by about 10%. The control strategy with a quasi-Z source net is also designed to obtain the adjustable commutation voltage in [28]. A non-inductive voltage regulating structure is presented to control the dc-link voltage in [29]. The proposed structure can suppress the commutation torque ripple and is applicable in a wide speed range. In [30], the two modes of a Cuk converter is adopted to regulate the dc-bus voltage in the non-commutation and commutation period, respectively. The proposed method reduces the commutation torque ripple and the voltage spike damage to the motor windings. The previous methods reduce the commutation torque ripple and shorten the commutation time. However, the DC/DC converters deliver the entire power in the commutation period, which increases the rated capacity of the power components and reduces reliability of electronic device.

In this paper, a suppression method based on an auxiliary step-up circuit is proposed to reduce the commutation torque ripple for BLDCM drive system. The auxiliary step-up circuit is composed of a capacitor, a transformer and a switch circuit. For effective suppression of the commutation toque ripple, the capacitor charged in the non-commutation period is connected in series with the power source to boost the dc-bus voltage, and then the dc-bus voltage is regulated by the three-phase inverter to meet the input voltage requirement of the motor. Compared the method based on the DC/DC inverter, the rated capacity of the power device is lowered. Since the additional energy is returned to the power source in each switching cycle, the utilization rate of the energy is improved. Moreover, the commutation time is shortened.

The rest of the paper is arranged as follows. Section 2 presents the causes of the commutation torque ripple. Section 3 discusses the operation principle of the proposed method and presents the desirable voltage for the charged capacitor. Section 4 presents the experimental implementation of the proposed method to verify the method's feasibility. Section 5 provides the conclusions.

II. ANALYSIS OF COMMUTATION TORQUE RIPPLE

The block diagram of BLDCM system is shown in Fig.1. In this paper, BLDCM operates in two-phase conduction mode and commutates current with the conventional six-step method.

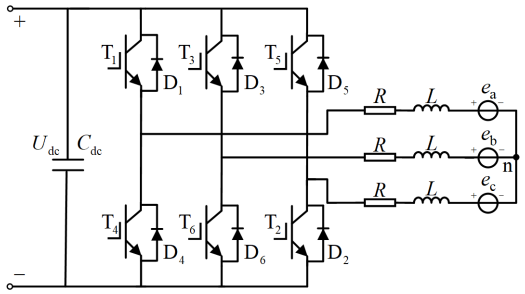

FIGURE 1. Block diagram of BLDCM drive system.

A. MATHEMATICAL MODEL OF BLDCM

Assuming that three-phase stator windings are symmetrical, the resistance and inductance are constant, and the armature reaction is negligible. The voltage equations are described as

$$\begin{bmatrix} u_a \\ u_b \\ u_c \end{bmatrix} = \begin{bmatrix} R & 0 & 0 \\ 0 & R & 0 \\ 0 & 0 & R \end{bmatrix} \begin{bmatrix} i_a \\ i_b \\ i_c \end{bmatrix} + \begin{bmatrix} L & 0 & 0 \\ 0 & L & 0 \\ 0 & 0 & L \end{bmatrix} \frac{d}{dt} \begin{bmatrix} i_a \\ i_b \\ i_c \end{bmatrix} + \begin{bmatrix} e_a \\ e_b \\ e_c \end{bmatrix} + \begin{bmatrix} u_n \\ u_n \\ u_n \end{bmatrix} \quad (1)$$

where u_a, u_b, and u_c are phase voltages, i_a, i_b, and i_c are phase currents, e_a, e_b, and e_c are phase back EMFs, R is the phase resistance, L is the phase inductance, and u_n is the neutral voltage of the motor.

The general equation of the torque is expressed as

$$T_e = \frac{e_a i_a + e_b i_b + e_c i_c}{\Omega} \quad (2)$$

where Ω is the mechanical angular velocity.

B. CAUSE OF COMMUTATION TORQUE RIPPLE

To analyze the cause of the commutation torque ripple, the commutation process from phase A to B is considered. When the commutation occurs, T_1 is turned off, T_3 is turned on, and T_2 remains on. The equivalent circuit is shown in Fig.2.

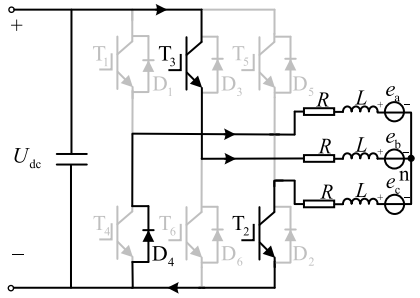

FIGURE 2. Equivalent circuit in the commutation process from phase A to B.

Considering a very small period of PWM, the phase current is regarded to be constant and equal to I. The phase current satisfies $i_a = -i_c = I$, and the back EMF meets $e_a = E$ and $e_c = -E$, where E donates the amplitude of the back EMF at the beginning of the commutation period. By substituting the back EMF and phase current into (2), the equation can be rewritten as

$$T_{e1} = \frac{e_a i_a + e_b i_b + e_c i_c}{\Omega} = \frac{2EI}{\Omega} \quad (3)$$

In the commutation process, the three-phase voltage meets $u_a = 0$, $u_b = U_{dc}$, and $u_c = 0$. Substituting the voltage function into (1), (1) is shown as

$$\begin{cases} u_a = Ri_a + L\dfrac{di_a}{dt} + e_a + u_n = 0 \\ u_b = Ri_b + L\dfrac{di_b}{dt} + e_b + u_n = U_{dc} \\ u_c = Ri_c + L\dfrac{di_c}{dt} + e_c + u_n = 0 \end{cases} \quad (4)$$

When the switching period of PWM is much shorter than the electrical time constant L/R, the effect of the phase resistance R is negligible. In general, the motor commutation time is relatively short, and thus it is assumed that the back EMF remains constant in the commutation period. The back EMF and phase current in the commutation period meet the functions:$e_a = e_b = -e_c = E$ and $i_a + i_b + i_c = 0$. By substituting the analysis into (4), and three-phase current expressions are solved as

$$\begin{cases} i_a = I - \dfrac{(U_{dc} + 2E)}{3L}t \\ i_b = \dfrac{2(U_{dc} - E)}{3L}t \\ i_c = -I - \dfrac{(U_{dc} - 4E)}{3L}t \end{cases} \quad (5)$$

Substituting (5) into (2), and the torque in the commutation period is shown as

$$T_{e2} = \frac{2E}{\Omega}\left(I + \frac{U_{dc} - 4E}{3L}t\right) \quad (6)$$

From (3) and (6), the torque ripple in the commutation period can be expressed as

$$\Delta T_e = T_{e1} - T_{e2} = \frac{2E(U_{dc} - 4E)}{3\Omega L}t \quad (7)$$

From (7), it is concluded that when the power source voltage is equal to four times back EMF amplitude, the torque before and after commutation remains constant.

III. PROPOSED METHOD TO SUPPRESS COMMUTATION TORQUE RIPPLE

The block diagram of BLDCM drive system is shown in Fig.3 and the auxiliary step-up circuit is marked by the dotted line. The auxiliary step-up circuit is composed of a capacitor C_1, a switch circuit (S_1 and S_2) and a transformer T_1. During the non-commutation period, the capacitor C_1 is charged up to the desired voltage U_e in accordance with the motor speed and back EMF. When the commutation starts, the capacitor C_1 is connected in series with the power source, and then three-phase inverter is regulated to ensure that the

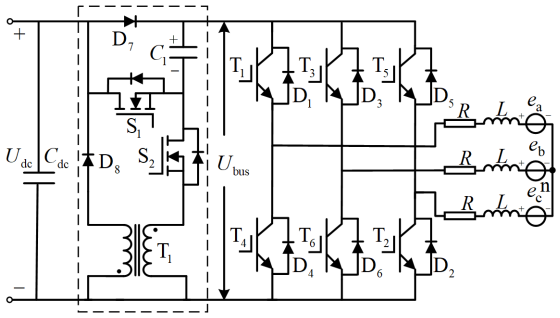

FIGURE 3. Configuration of BLDCM drive system with the proposed auxiliary step-up circuit.

input voltage of the motor is equal to four times back EMF amplitude. The operation principle of the proposed method will be analyzed as follows.

A. OPERATION PRICIPLE OF PROPOSED METHOD

To facilitate the analysis, the conduction period of phase AC is considered. During the conduction period of phase AC, the switch S_1 is turned off, and the capacitor C_1 is charged by regulating the switch S_2. When the switch S_2 is on, the start of all windings on the transformer T_1 will go positive and the current in the primary will be built up. Meanwhile, the capacitor C_1 is charged and the capacitor voltage begins to rise, the charging equivalent circuit is shown in Fig.4(a). When the switch S_2 is off, the charging process is interrupted, and the capacitor voltage remains constant. Meanwhile, the energy stored in the transformer is returned to the power source, and the equivalent circuit is shown in Fig.4(b). Continue to regulate the switch S_2 until the capacitor voltage reaches the desired value U_e. Then the switch S_2 is turned off and the charging process is over.

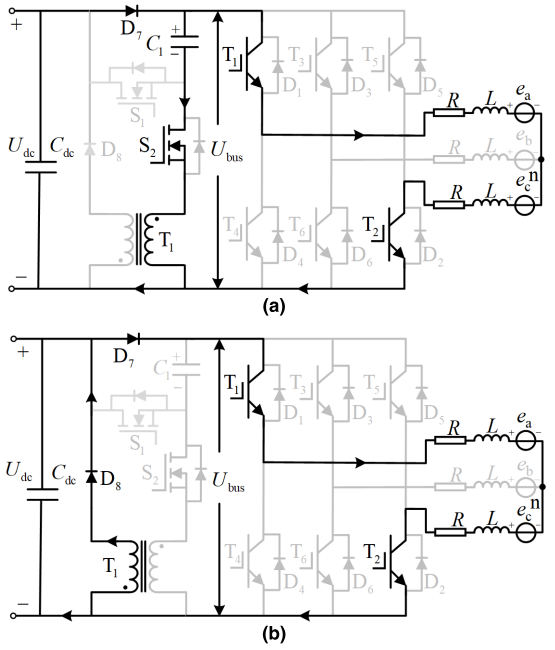

FIGURE 4. Equivalent circuit of the capacitor charging process in the conduction period of phase A and C. (a) Switch S_1 is OFF while Switch S_2 is ON. (b) Switch S_1 is OFF while Switch S_2 is OFF.

When the commutation begins, the switch S_1 is turned on and the switch S_2 is turned off. The diode D_7 is blocked and the charged capacitor C_1 is instantly added on the power source U_{dc} to step up the dc-bus voltage U_{bus}, the equivalent circuit is shown in Fig.5. The corresponding power devices of the three-phase inverter are then regulated to ensure that the input voltage of the motor is equal to four times back EMF for the commutation torque ripple suppression. When the commutation process is finished, the charged capacitor C_1 is removed from the dc-bus voltage with the switch circuit, and then the charging resumes.

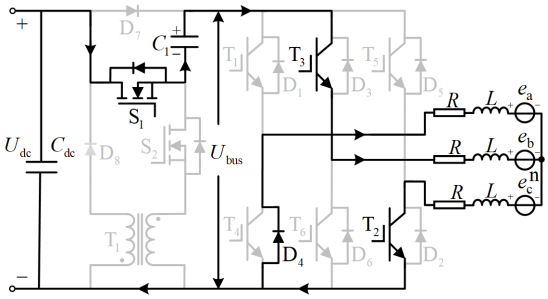

FIGURE 5. The equivalent circuit in the commutation period.

B. DESIRED CHARGED VOLTAGE

Fig.6 shows the variation of the capacitor voltage in the 60 electrical period with the proposed method. Before the commutation begins, the dc-bus voltage U_{bus} keeps at the level of U_α. During the commutation period, the capacitor voltage declines as it supplies the motor, and the dc-bus voltage U_{bus} drops along the line "1." When the commutation time t_{com} is over, the dc-bus voltage U_{bus} drops to U_β. The voltage drop of the capacitor is denoted by ΔU during the commutation process. The capacitor is then charged upon entering the non-commutation period. Consequently, the capacitor voltage increases, and the dc-bus voltage U_{bus} begins to rise along the line "2." When the capacitor voltage reaches the desirable value U_e, the dc-bus voltage U_{bus} remains constant along the line "3", then the charging course terminates. To ensure the

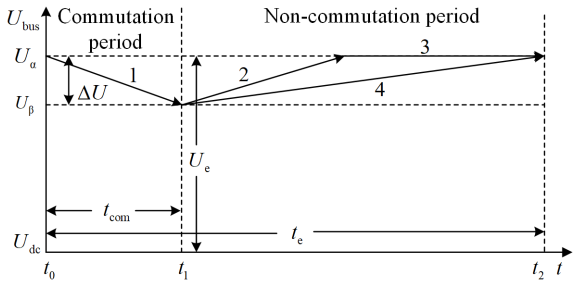

FIGURE 6. Variation of capacitor voltage in 60° electrical period.

effective implementation of the proposed method, the capacitor voltage should reach the desirable value before the beginning of the commutation period. In the critical situation, the capacitor voltage reaches the desirable value U_e exactly at the end of the non-commutation period. It means that the dc-bus voltage increases along the line "4."

During the commutation period, the capacitor and power source supply the motor; hence, it is reasonable that the sum of the energy released by both equals the energy consumed by the motor in the commutation period. Assuming the amplitude of the noncommutative phase current remains constant and the resistance loss is negligible, according to the energy conservation law,

$$W_{\text{disch}} = \frac{1}{2} C_{\text{eqv}} \left[U_\alpha^2 - U_\beta^2 \right] = 2EI \cdot t_{\text{com}} \tag{8}$$

where $C_{\text{eqv}} = C_1 \cdot C_{\text{dc}} / (C_1 + C_{\text{dc}})$, t_{com} is the commutation time, and $U_\alpha = U_\beta + \Delta U$.

In [25], the commutation time $t_{\text{com}} = LI/2E$. As seen in Fig.6, $U_\alpha = U_\beta + \Delta U$. By substituting the aforementioned analysis into (8), and the capacitor voltage variation ΔU can be given as

$$\Delta U = \sqrt{\frac{2LI^2}{C_{\text{eqv}}} + U_\beta^2} - U_\beta \tag{9}$$

Given that the desirable voltage U_e satisfies $U_e = U_\beta - U_{\text{dc}} + \Delta U$, and the desirable voltage U_e can be expressed as

$$U_e = \sqrt{\frac{2LI^2}{C_{\text{eqv}}} + U_\beta^2} - U_{\text{dc}} \tag{10}$$

To reduce the commutation torque ripple during the commutation period, the dc-bus voltage at the end of the commutation period should meet $U_{\text{bus}} \geqslant 4E$. In this study, the dc-bus voltage value U_β at the end of commutation period is chosen as $U_\beta = 4E$. Therefore, the desirable voltage U_e can be updated as

$$U_e = U_\beta - U_{\text{dc}} + \Delta U = \sqrt{\frac{2LI^2}{C_{\text{eqv}}} + 16E^2} - U_{\text{dc}} \tag{11}$$

IV. EXPERIMENT RESULT

The experimental prototype is set up to verify the feasibility and effectiveness of the proposed method. Fig.7 shows the experimental platform and it consists of the control system and the experimental motor. The motor is connected to the generator by a flexible coupling. The rated parameters of BLDCM are shown in Table 1. The core processor is DSP controller (TMS320F28335) with 150MHz clock frequency, and the three-phase inverter is composed of IPM PM50RL1A060 (Mitsubishi). The capacitance value of the capacitor $C_1$is designed as 60μF, and it is composed of two 30μF non-inductance capacitors with parallel connections. The capacitor C_1 voltage U_{c1} is sampled with the voltage sensor (LV25-P) and the sampling frequency of the voltage is 20kHz. The dc-bus current i_{dc} is sampled with the current sensor (LTS15-NP) and the sampling frequency of the current

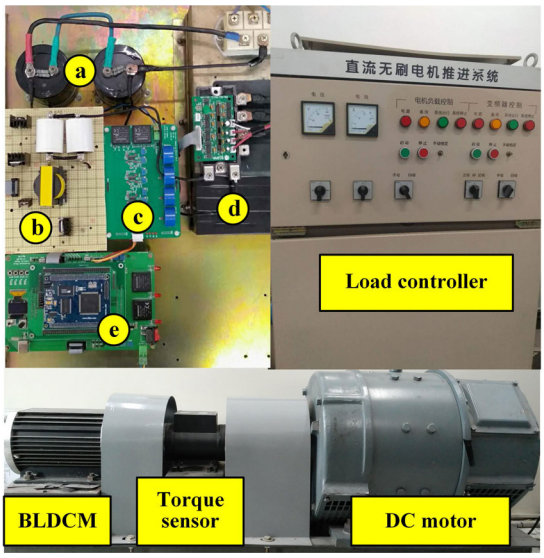

FIGURE 7. Platform of BLDCM experimental system. (a) Bus capacitor. (b) Proposed auxiliary step-up circuit. (c) Sampling board. (d) Main circuit. (e) Control board.

TABLE 1. Main parameters in the experiment.

Motor parameters	Value	Unit
Rated voltage	200	V
Rated power	3.2	kW
Rated speed	1500	rpm
Rated torque	20	Nm
Pole pairs	4	
Phase inductance	1.234	mH
Back EMF coefficient	0.528	V/(rad/s)
Primary inductance	0.97	mH
Capacitor capacitance	60	μF

is 10kHz. The switching frequency of S_2 is 20kHz, and the duty ratio is 0.5. The modulation method of the three-phase inverter is PWM-ON, and the switching frequency of the three-phase inverter is 10kHz. The torque and speed are measured by the torque sensor. The experimental results are monitored and recorded by a digital oscilloscope DL750 (YOKOGAWA). The block diagram of the system control is shown in Fig.8.

In the implementation process, BLDCM drive system is controlled with the traditional double-loop PI regulators (i.e., the speed loop and the current loop). The charged voltage U_{c1} of the capacitor C_1 is sampled with the voltage sensor, the dc-bus current i_{dc} is sampled with the current sensor and the two sampled signals are sent to DSP controller. The hall signals are monitored by DSP controller to estimate the motor speed ω and judge the working state of the motor. When the motor works in the non-commutation period, DSP controller sends control signals to turn off S_1 and regulate $S_2$with a fixed duty cycle of 50% for charging the capacitor C_1. When the capacitor voltage reaches the

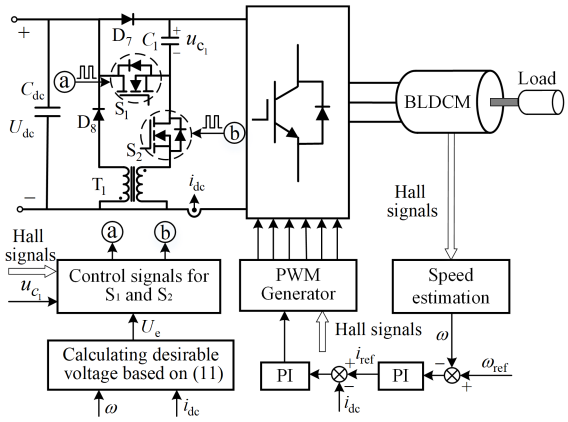

FIGURE 8. Configuration of the proposed BLDCM control system.

desirable voltage U_e, DSP controller sends control signals to turn off S_2, the charging process is over. When the motor works in the commutation period, DSP controller sends control signals to turn on S_1 for t_{com}. Then S_1 is turned off, and the commutation period is completed [31], [32]. The flow chart is shown in Fig.9.

The torque ripple is defined as

$$K_r = \frac{T_{P\text{-}P}}{T_{Avg}} \times 100\%$$

where $T_{P\text{-}P}$ is the peak-peak value of torque and T_{Avg} is the average torque.

In these experiments, three control methods are used to compare the performance. In the conventional method, the ON-PWM modulation method is used to regulate the three-phase inverter of BLDCM. In the second method, the SEPIC converter is placed in front of the three-phase inverter to regulate the dc-bus voltage during the commutation period. In the third method, the proposed method is applied to reduce the torque ripple in the commutation period.

Fig.10-12 show the comparative results of the three control methods under different speed and load conditions, (the right side of each experimental result is its enlarged view). Fig.10 shows the experimental results of three control methods with the rated speed and load torque. Fig.10(a) shows the experimental results when the conventional method is used. In Fig.10(a), the dc-bus voltage U_{bus} remains constant in the commutation period, there exists a remarkable torque pulsation and the torque ripple $K_r \approx 35.3\%$. Moreover, the commutation time is relatively long and the commutation time $t \approx 296\mu$s. Fig.10(b) shows the experimental results with the SEPIC converter. In Fig.10(b), the dc-bus voltage U_{bus} remains at $4E$ in the commutation process, the torque ripple K_r drops to about 12.8% and the commutation time $t \approx 189\mu$s, where E denotes the amplitude of back EMF. Fig.10(c) shows the experimental results with the proposed method. It is observed that the dc-bus voltage U_{bus} boosts at the beginning of the commutation period and gradually declines in the commutation period. When the commutation

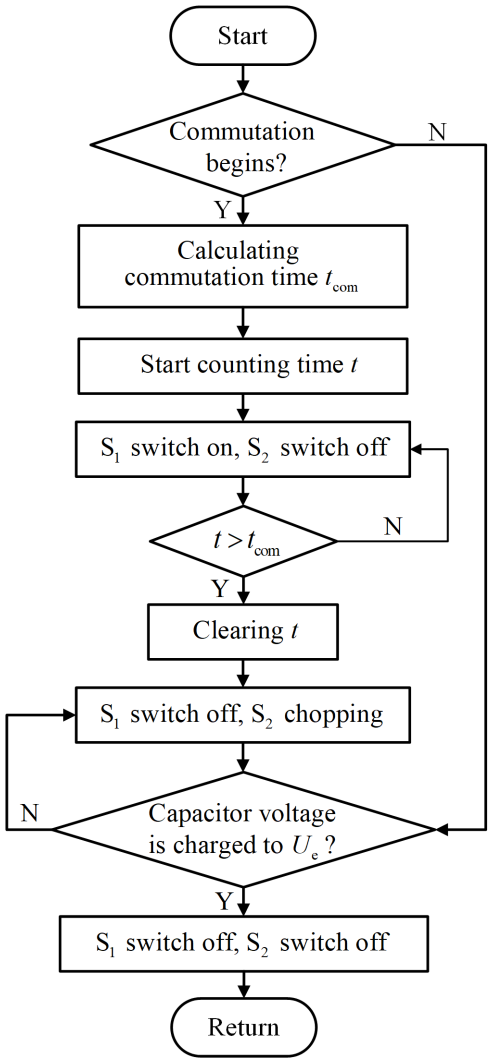

FIGURE 9. Flowchart of the proposed method.

is over, the dc-bus voltage remains at about $4E$, the torque ripple $K_r \approx 12.8\%$ and the commutation time $t \approx 189\mu$s. In addition, the voltage variation ΔU is 41V, and it approximately agrees with (9). Compared with the experimental results with the conventional method, it can be found that the torque ripple and commutation time are obviously reduced when the SEPIC converter and the proposed method are used. Moreover, the torque ripple and the commutation time of the proposed method are slightly less than that of the SEPIC converter.

Fig.11 illustrates the experimental results of three control methods with the high speed and 50% rated load torque, and Fig.12shows comparative results with the rated speed and 25% rated load torque. In the two groups of experiments, the torque ripple and commutation time are effectively reduced compared with the conventional method. Moreover, the proposed method performs slightly better than the SEPIC converter in terms of the torque ripple and commutation time. Table 2 summarizes the comparative results of the

TABLE 2. Comparison of three control methods.

Speed (rpm)	Torque (Nm)	Conventional Method		SEPIC Converter Method		Proposed Method	
		Torque ripple K_r	Com.time t_{com}	Torque ripple K_r	Com.time t_{com}	Torque ripple K_r	Com.time t_{com}
1500	20	35.3%	296μs	17.4%	201μs	12.8%	189μs
1200	10	25.4%	159μs	11.3%	145μs	7.9%	136μs
1500	5	38.2%	90μs	26.4%	71μs	25.3%	66μs

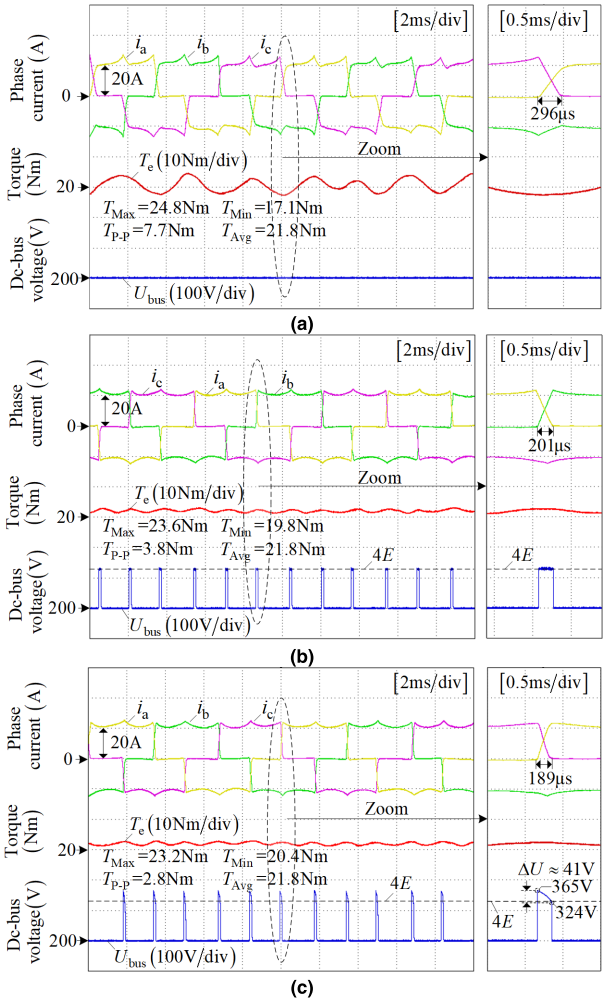

FIGURE 10. Experimental results under a speed of 1500rpm and a load torque of 20Nm. (a) Conventional method. (b) SEPIC converter. (c) Proposed method.

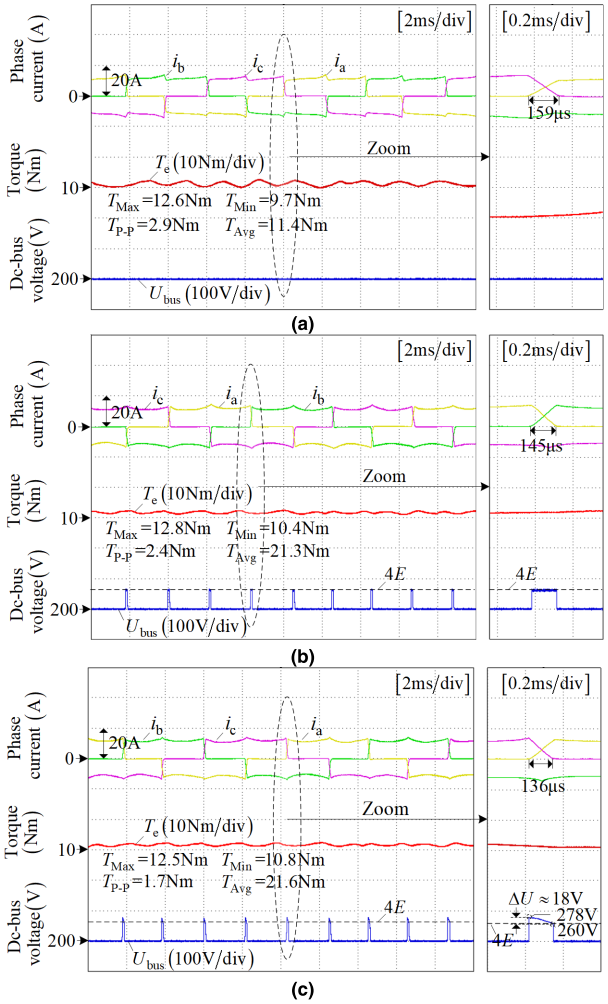

FIGURE 11. Experimental results under a speed of 1200rpm and a load torque of 10Nm. (a) Conventional method. (b) SEPIC converter. (c) Proposed method.

three methods under various speeds and torque loads. From the comparative results, it is seen that there exists obvious commutation torque ripple with the conventional method, and the commutation time is relatively long. However, when the proposed method is used to boost the dc-bus voltage in the commutation period, the commutation torque ripple and commutation time are evidently reduced. Under these two speed and load conditions, the voltage variation ΔU and the dc-bus voltage U_{bus} at the end of the commutation period are also basically consistent with (9) and $4E$, respectively. Therefore, the proposed method shows the satisfactory steady-state performance under different conditions.

For comparison, the method based on the SEPIC converter is also tested, and the test results show that the SEPIC converter and the proposed method can reduce the commutation torque ripple and shorten the commutation time, and the proposed method demonstrates a slight advantage over the SEPIC converter method. For the SEPIC converter method, the power components provide the full power for BLDCM in the commutation period. But the proposed auxiliary step-up circuit only provides partial power required in the commutation process of the motor, which reduces the devices capacity and improves the system reliability.

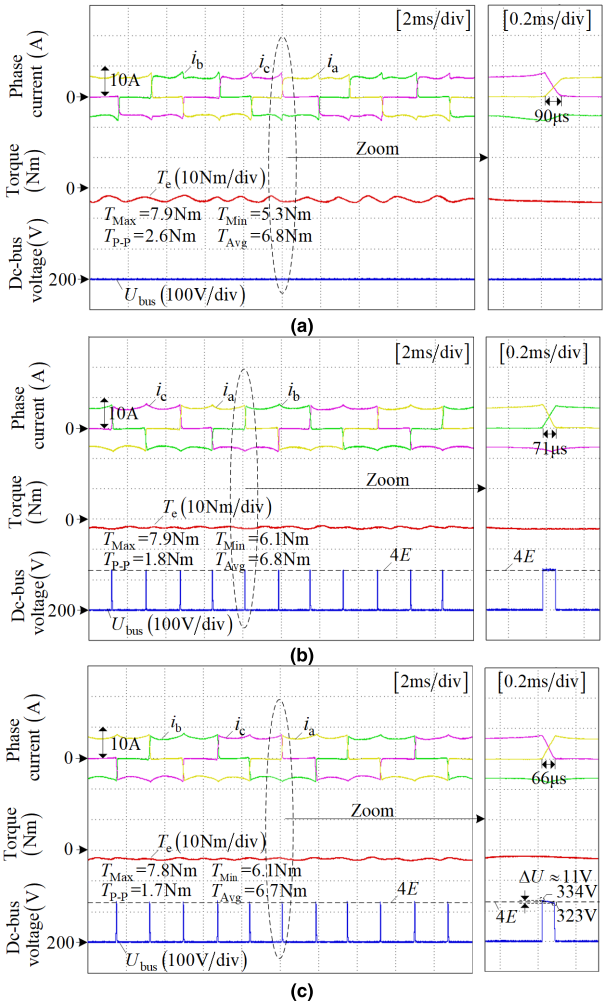

FIGURE 12. Experimental results under a speed of 1500rpm and a load torque of 5Nm. (a) Conventional method. (b) SEPIC converter. (c) Proposed method.

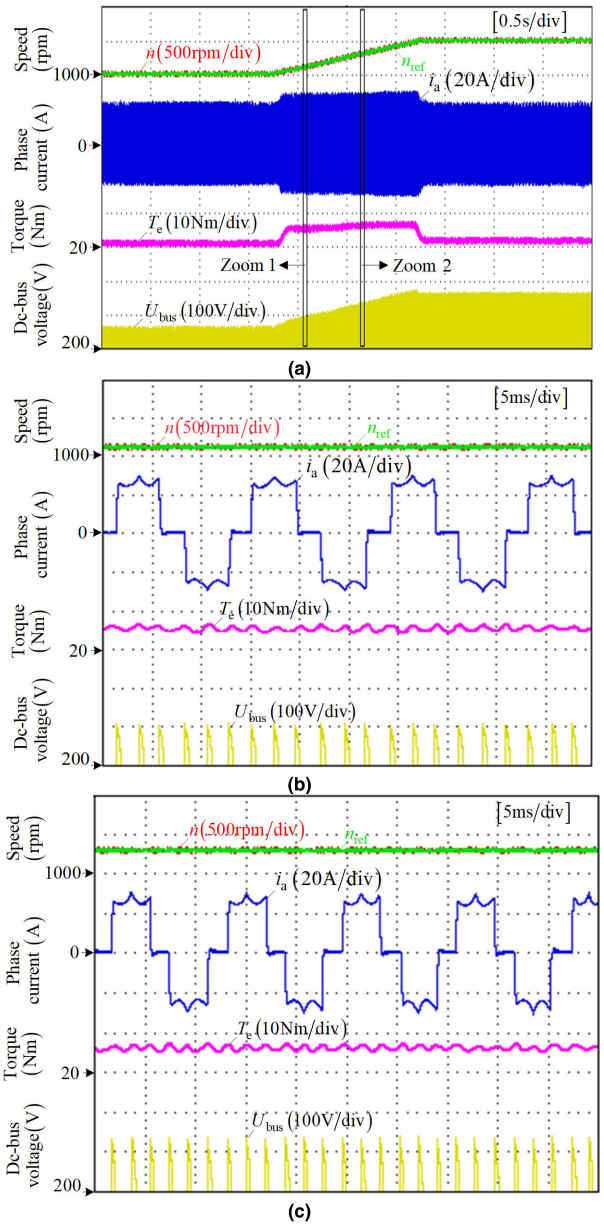

FIGURE 13. Dynamic response of speed variation with the proposed method. (a) Speed, current, electromagnetic torque and dc-bus voltage. (b) Zoom 1. (c) Zoom 2.

To verify the dynamic performance of the proposed method, the experiments under the variable speed and load are performed. Fig.13(a), (b) and (c) show the variable speed performance of the proposed method and the enlarged views. The reference speed n_{ref} follows a ramp function in the experiment. Before the motor accelerates, the speed is 1000rpm and load torque is 20Nm. During the acceleration process, the reference speed n_{ref} rises with a slope function, and the motor accelerates from 1000rpm to 1500rpm within 2 s. As seen in Fig.13(a), the actual speed n can accurately track the reference speed n_{ref}. The phase current i_a and the electromagnetic torque T_e slightly increase, and the dc-bus voltage U_{bus} correspondingly increases to suppress the commutation torque ripple. Fig.13(b) and (c) show the enlarged views under speeds of 1100rpm and 1300rpm, respectively. It can be observed that the phase current fluctuation is not evident, and the commutation torque ripple still can be effectively reduced. Experimental results show that the proposed method is effective under the condition of variable speed operation.

Fig.14(a), (b) and (c) show the variable load results of the proposed method and the enlarged views. Before the load torque varies, the motor speed n is about 1500rpm and the electromagnetic torque T_e is about 10Nm. During the variable load experiment, the load torque command T_L varies from 10 Nm to 20Nm. It is found from Fig.14(a) that the phase current increases with the variation of the load torque, and the dc-bus voltage slightly rises to maintain the commutation torque steady. Fig.14(b) and (c) show the enlarged views when the electromagnetic torques are 13 and 15 Nm, respectively. The results show that the phase current and the torque in the commutation period remain steady, and no significant fluctuation is observed. In conclusion, the proposed method exhibits the good dynamic performance.

Fig.15 shows the harmonic analysis results with the conventional method and the proposed method under a speed 1500rpm and the load torque of 20Nm. The harmonic

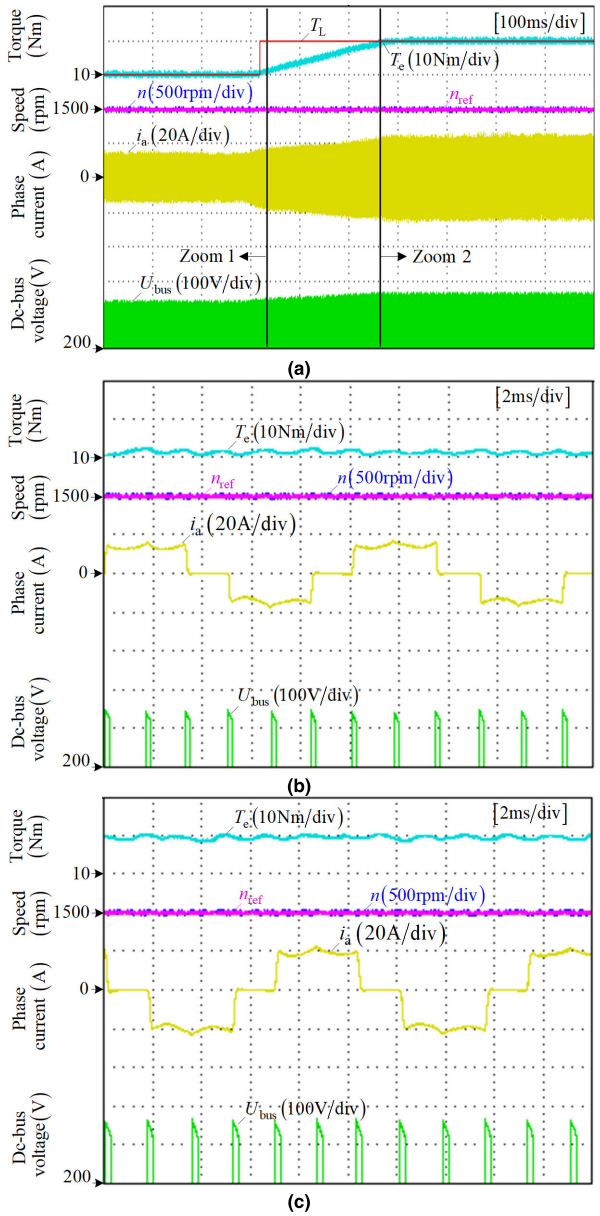

FIGURE 14. Dynamic response of load torque variation with the proposed method. (a) Electromagnetic torque, speed, current, and dc-bus voltage. (b) Zoom 1. (c) Zoom 2.

components of the commutation torque ripple are mainly concentrated on 6 $nf(n = 1, 2, 3\ldots)$. When the motor speed is 1500rpm, the fundamental frequency is $f = 1500p/60 = 100$ Hz. In the conventional method, the integer times harmonic component of $6f$ is higher, and the harmonic amplitudes at $6f$ and $12f$ are 1.70 and 0.59, respectively. With the proposed method, the integer times harmonic component of $6f$ is reduced, and the harmonic amplitudes at $6f$ and $12f$ are 0.53 and 0.13, respectively. Compared with the conventional method, the harmonic amplitudes are reduced by about 68.8% and 77.9%, respectively. The experimental results show that the proposed method has the ability to suppress the commutation torque ripple effectively.

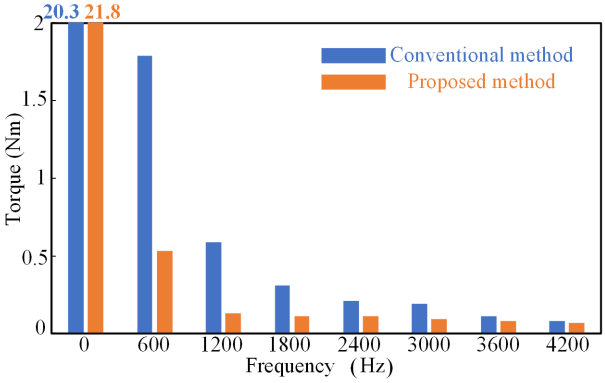

FIGURE 15. Harmonic spectra of torque with a speed of 1500rpm and a load torque of 20Nm.

V. CONCLUSION

In this study, an auxiliary step-up circuit is presented to suppress the commutation torque ripple of BLDCM. First, the cause of the commutation torque ripple is given, and the condition of restraining the torque ripple is derived. Then, the operation principle of the proposed method is provided. The charging process in the non-commutation period and the booting principle in the commutation period are analyzed in detail. The desirable charged voltage is designed with a graphical method, and thus the design process is simplified. To verify the steady-state performance of the proposed boost structure, three sets of comparative experiments are carried out under different working conditions, and the results demonstrate the feasibility of the proposed method. In each group of experiments, the conventional method, the SEPIC converter method and the proposed method are tested to compare the torque ripple and the commutation interval. The results show that latter two methods can obviously suppress the commutation torque ripple and shorten the commutation time compared with the conventional method. In addition, the proposed method performs slightly better than the SEPIC converter method, and the voltage stress of the power device in the proposed method is evidently lower than that of the SEPIC converter method since the power components in the proposed method only deliver a portion of the energy required during the commutation interval. The variable speed and load experiments are conducted, and the results indicates that the proposed method has fast dynamic response. The harmonic components in the torque is one of the important factors causing the motor mechanical vibration. In this study, the torque spectra analysis is conducted for the conventional method and proposed method. The experimental results show that the harmonic components of 6 nf with the proposed method are obviously weakened compared with that of the conventional method.

REFERENCES

[1] Z. Q. Zhu and J. H. Leong, "Analysis and mitigation of torsional vibration of PM brushless AC/DC drives with direct torque controller," *IEEE Trans. Ind. Appl.*, vol. 48, no. 4, pp. 1296–1306, Jul./Aug. 2012.

[2] X. Huang, A. Goodman, C. Gerada, Y. Fang, and Q. Lu, "A single sided matrix converter drive for a brushless DC motor in aerospace applications," *IEEE Trans. Ind. Electron.*, vol. 59, no. 9, pp. 3542–3552, Sep. 2012.
[3] X. Sun, C. Hu, J. Zhu, S. Wang, W. Zhou, Z. Yang, G. Lei, K. Li, B. Zhu, and Y. Guo, "MPTC for PMSMs of EVs with multi-motor driven system considering optimal energy allocation," *IEEE Trans. Magn.*, vol. 55, no. 7, Jul. 2019, Art. no. 8104306.
[4] T.-W. Chun, Q.-V. Tran, H.-H. Lee, and H.-G. Kim, "Sensorless control of BLDC motor drive for an automotive fuel pump using a hysteresis comparator," *IEEE Trans. Power Electron.*, vol. 29, no. 3, pp. 1382–1391, Mar. 2014.
[5] X. Sun, C. Hu, G. Lei, Y. Guo, and J. Zhu, "State feedback control for a PM hub motor based on grey wolf optimization algorithm," *IEEE Trans. Power Electron.*, to be published. doi: 10.1109/TPEL.2019.2923726.
[6] L. I. Iepure, I. Boldea, and F. Blaabjerg, "Hybrid I-f starting and observer-based sensorless control of single-phase BLDC-PM motor drives," *IEEE Trans. Ind. Electron.*, vol. 59, no. 9, pp. 3436–3444, Sep. 2012.
[7] Z. Shi, X. Sun, Y. Cai, Z. Yang, G. Lei, Y. Guo, and J. Zhu, "Torque analysis and dynamic performance improvement of A PMSM for EVs by skew angle optimization," *IEEE Trans. Appl. Supercond.*, vol. 29, no. 2, Mar. 2019, Art. no. 0600305.
[8] J. Zou, W. Qi, Y. Xu, F. Xu, and J. Li, "Design of deep sea oil-filled brushless DC motors considering the high pressure effect," *IEEE Trans. Magn.*, vol. 48, no. 11, pp. 4220–4223, Nov. 2012.
[9] J. H. Song and I. Choy, "Commutation torque ripple reduction in brushless DC motor drives using a single DC current sensor," *IEEE Trans. Power Electron.*, vol. 19, no. 2, pp. 312–319, Mar. 2004.
[10] J. Fang, H. Li, and B. Han, "Torque ripple reduction in BLDC torque motor with non-ideal back EMF," *IEEE Trans. Power Electron.*, vol. 27, no. 11, pp. 4630–4637, Nov. 2012.
[11] J. Shi and T.-C. Li, "New method to eliminate commutation torque ripple of brushless DC motor with minimum commutation time," *IEEE Trans. Ind. Electron.*, vol. 60, no. 6, pp. 2139–2146, Jun. 2013.
[12] C. Xia, Y. Xiao, W. Chen, and T. Shi, "Torque ripple reduction in brushless DC drives based on reference current optimization using integral variable structure control," *IEEE Trans. Ind. Electron.*, vol. 61, no. 2, pp. 738–752, Feb. 2014.
[13] D.-K. Kim, K.-W. Lee, and B.-I. Kwon, "Commutation torque ripple reduction in a position sensorless brushless DC motor drive," *IEEE Trans. Power Electron.*, vol. 21, no. 6, pp. 1762–1768, Nov. 2006.
[14] C. Xia, Y. Wang, and T. Shi, "Implementation of finite-state model predictive control for commutation torque ripple minimization of permanent-magnet brushless DC motor," *IEEE Trans. Ind. Electron.*, vol. 60, no. 3, pp. 896–905, Mar. 2013.
[15] W. Jiang, H. Huang, J. Wang, Y. Gao, and L. Wang, "Commutation analysis of brushless DC motor and reducing commutation torque ripple in the two-phase stationary frame," *IEEE Trans. Power Electron.*, vol. 32, no. 6, pp. 4675–4682, Jun. 2017.
[16] M. S. Boroujeni, G. A. Markadeh, J. Soltani, and F. Blaabjerg, "Torque ripple reduction of brushless DC motor with harmonic current injection based on integral terminal sliding mode control," *IET Electr. Power Appl.*, vol. 12, no. 1, pp. 25–36, Jan. 2018.
[17] H. Lu, L. Zhang, and W. Qu, "A new torque control method for torque ripple minimization of BLDC motors with un-ideal back EMF," *IEEE Trans. Power Electron.*, vol. 23, no. 2, pp. 950–958, Mar. 2008.
[18] Y. Liu, Z. Q. Zhu, and D. Howe, "Commutation-torque-ripple minimization in direct-torque-controlled PM brushless DC drives," *IEEE Trans. Ind. Appl.*, vol. 43, no. 4, pp. 1012–1021, Jul. 2007.
[19] Y. Zhou, D. Zhang, X. Chen, and Q. Lin, "Sensorless direct torque control for saliency permanent magnet brushless DC motors," *IEEE Trans. Energy Convers.*, vol. 31, no. 2, pp. 446–454, Jun. 2016.
[20] K. D. Carey, N. Zimmerman, and C. Ababei, "Hybrid field oriented and direct torque control for sensorless BLDC motors used in aerial drones," *IET Power Electron.*, vol. 12, no. 3, pp. 438–449, Mar. 2019.
[21] T. Shi, Y. Cao, G. Jiang, X. Li, and C. Xia, "A torque control strategy for torque ripple reduction of brushless DC motor with nonideal back electromotive force," *IEEE Trans. Ind. Electron.*, vol. 64, no. 6, pp. 4423–4433, Jun. 2017.
[22] T. Sheng, X. Wang, J. Zhang, and Z. Deng, "Torque-ripple mitigation for brushless DC machine drive system using one-cycle average torque control," *IEEE Trans. Ind. Electron.*, vol. 62, no. 4, pp. 2114–2122, Apr. 2015.
[23] Z. Xiaofeng and L. Zhengyu, "A new BLDC motor drives method based on BUCK converter for torque ripple reduction," in *Proc. IEEE Power Electron. Motion Control, Conf.*, Aug. 2006, pp. 1–4.
[24] H.-J. Hu, G.-Z. Cao, S.-D. Huang, C. Wu, and Y.-P. Peng, "Drive circuit-based torque-ripple suppression method for single-phase BLDC fan motors to reduce acoustic noise," *IET Electr. Power Appl.*, vol. 13, no. 7, pp. 881–888, Jul. 2019.
[25] T. Shi, Y. Guo, P. Song, and C. Xia, "A new approach of minimizing commutation torque ripple for brushless DC motor based on DC–DC converter," *IEEE Trans. Ind. Electron.*, vol. 57, no. 10, pp. 3483–3490, Oct. 2010.
[26] V. Viswanathan and J. Seenithangom, "Commutation torque ripple reduction in the BLDC motor using modified SEPIC and three-level NPC inverter," *IEEE Trans. Power Electron.*, vol. 33, no. 1, pp. 535–546, Jan. 2018.
[27] X. Li, C. Xia, Y. Cao, W. Chen, and T. Shi, "Commutation torque ripple reduction strategy of Z-source inverter fed brushless DC motor," *IEEE Trans. Power Electron.*, vol. 31, no. 11, pp. 7677–7690, Nov. 2016.
[28] K. Xia, J. Lu, C. Bi, Y. Tan, and B. Dong, "Dynamic commutation torque-ripple reduction for brushless DC motor based on quasi-Z-source net," *IET Electr. Power Appl.*, vol. 10, pp. 819–826, Nov. 2016.
[29] G. Jiang, C. Xia, W. Chen, T. Shi, X. Li, and Y. Cao, "Commutation torque ripple suppression strategy for brushless DC motors with a novel noninductive boost front end," *IEEE Trans. Power Electron.*, vol. 33, no. 5, pp. 4274–4284, May 2018.
[30] W. Chen, Y. Liu, X. Li, T. Shi, and C. Xia, "A novel method of reducing commutation torque ripple for brushless DC motor based on Cuk converter," *IEEE Trans. Power Electron.*, vol. 32, no. 27, pp. 5497–5508, Jul. 2017.
[31] X. Sun, K. Diao, G. Lei, Y. Guo, and J. Zhu, "Study on segmented-rotor switched reluctance motors with different rotor pole numbers for BSG system of hybrid electric vehicles," *IEEE Trans. Veh. Technol.*, vol. 68, no. 6, pp. 5537–5547, Jun. 2019.
[32] X. Sun, K. Diao, G. Lei, Y. Guo, and J. Zhu, "Real-time HIL emulation for a segmented-rotor switched reluctance motor using a new magnetic equivalent circuit," *IEEE Trans. Power Electron.*, to be published. doi: 10.1109/TPEL.2019.2933664.

XULIANG YAO received the Ph.D. degree from the College of Automation, Harbin Engineering University, Harbin, China, in 2005, where he is currently a Professor. His current research interests include power electronics and power drive, ship electric propulsion, and control theory of shipping motion.

JICHENG ZHAO received the B.S. and M.S. degrees from the College of Automation, Harbin Engineering University, Harbin, China, in 2008 and 2011, respectively, where he is currently pursuing the Ph.D. degree. His current research interests include sensorless drive and commutation ripple suppression of BLDC.

JINGFANG WANG was born in Hebei, China, in 1984. He received the B.S. degree in automation from Yanshan University, Qinhuangdao, China, in 2008, the M.S. degree in electrical engineering from Harbin Engineering University, Harbin, China, in 2012, and the Ph.D. degree in electrical engineering from the Harbin Institute of Technology, Harbin, in 2017. Since 2017, he has been a Lecturer at the College of Automation, Harbin Engineering University. His research interests include high-power converters and harmonics compensation.

SHENGQI HUANG received the B.S. degree in electrical engineering and automation from Northeast Petroleum University, Daqing, China, in 2017. He is currently pursuing the Ph.D. degree with the College of Automation, Harbin Engineering University, Harbin, China. His research interests include control technology of PM machines and predictive control technology.

YISHU JIANG received the B.S. degree in electrical engineering from Northeast Agricultural University, Harbin, China, in 2016. She is currently pursuing the M.Sc. degree with the College of Automation, Harbin Engineering University, Harbin. Her research interest includes sensorless control technology of brushless DC motor.